



Investigation of alumina nanofiller impact on the structural and dielectric properties of PEO/PMMA blend matrix-based polymer nanocomposites

R. J. Sengwa¹ · Shobhna Choudhary^{1,2} · Priyanka Dhatarwal¹

Received: 3 November 2018 / Revised: 12 January 2019 / Accepted: 28 January 2019 / Published online: 8 February 2019
© Springer Nature Switzerland AG 2019

Abstract

Polymer nanocomposite (PNC) films have been prepared by the solution-cast method using a polymer blend of poly(ethylene oxide) (PEO) and poly(methyl methacrylate) (PMMA) (PEO/PMMA = 50/50 wt%) as organic host matrix and x wt% Al_2O_3 nanoparticles ($x = 0, 1, 3, \text{ and } 5$) as inorganic nanofiller. The morphological and structural behavior of these PNC films has been examined by employing the scanning electron microscope (SEM), X-ray diffractometer (XRD), and Fourier transform infrared (FTIR) spectrometer, whereas their dielectric polarization and relaxation processes are characterized by carrying out the dielectric relaxation spectroscopy (DRS) over the frequency range 2×10^1 to 1×10^6 Hz. Impact of Al_2O_3 nanofiller on the spherulite and porous morphology, degree of crystallinity, polymer-polymer and polymer-nanoparticle interactions, complex dielectric permittivity, ac electrical conductivity, and the polymers structural dynamics has been explored. It is revealed that initially 1 wt% dispersion of Al_2O_3 in the PEO/PMMA blend matrix significantly reduces the crystallinity and dielectric permittivity, and hinders the cooperative chain segmental dynamics of the polymers which unevenly changes with the further increase of Al_2O_3 concentration up to 5 wt%. The dielectric and electrical parameters of these materials have also been compared with the PNC materials based on other polar polymer host matrices containing different oxide inorganic nanoparticles. The results of this work provide a guideline to design and fabricate the alumina nanoparticles loaded flexible-type polymer nanodielectric materials for advanced technologies.

Keywords Polymer nanocomposites · Polymer blend · Dielectric properties · Structural dynamics · Nanodielectrics

1 Introduction

The degree of miscibility and structural dynamics in the polymers blend films consisted of semicrystalline poly(ethylene oxide) (PEO) and amorphous poly(methyl methacrylate) (PMMA) depends on the compositional ratio of these polymers in the blend films and also the film preparation methods [1–9]. These technologically important structural properties of the PEO/PMMA blend which can be tailored predominantly by taking into consideration the appropriate compositional

ratio have realized it as a novel, efficient, and cost-effective material as host matrix for the preparation of solid polymer electrolyte (SPE) films to be used as separator/ion conductor in the design and fabrication of flexible-type all-solid-state ion conducting devices [10–15], and also in the solar energy harvesting devices [16]. Besides the poor thermal and mechanical properties and a relatively high degree of crystallinity, the PEO is frequently used as a base matrix for the SPEs because of its high solvating power for the alkali metal salts and excellent flexible-type film forming ability [17]. Although the PMMA film is thermally more stable and has an almost amorphous structure which confirms its suitability as a host matrix for the SPEs [18, 19], it is less flexible and highly fragile when twisted or bent, restricting its vast technological applications in the flexible electronics. Hence, in order to suppress the individual drawbacks and the enhancement of their optimum useful properties, the PEO/PMMA blend as the base matrix is preferred for the preparation of technological important electrolyte materials [3, 10–16].

✉ R. J. Sengwa
rjsengwa@rediffmail.com; rjs.ph@jnvu.edu.in

¹ Dielectric Research Laboratory, Department of Physics, Jai Narain Vyas University, Jodhpur 342 005, India

² CSIR – National Institute of Science Communication and Information Resources, New Delhi 110 012, India

The compositional dependent investigation on the thermomechanical properties of PEO/PMMA blend matrices revealed that plasticization of the PMMA occurs by the presence of blended PEO which reduces its brittleness, whereas the mechanical and thermal stabilities of PEO are greatly improved by the simultaneous existence of PMMA in their blend matrix [3]. In addition to the overall improvement of the thermal and mechanical properties, the degree of crystallinity of the PEO greatly reduces on its blending with the PMMA [3, 6], and therefore the reduced crystalline phase of PEO/PMMA blend matrix promotes a large number of favorable paths for the ion transportation and hence this polymer blend is often considered as a novel host functional matrix for the SPE materials [3, 10–16, 20–22]. So far, various spectroscopic and thermomechanical investigations on the PEO/PMMA blends of various compositional ratios have established that a homogeneous and predominantly amorphous structure of this blend is formed for the PEO concentrations up to 30 wt%, whereas the blend miscibility gradually reduces as the PEO concentration exceeds above this critical limit [1–9]. Further, it has also been confirmed that the cooperative chain segmental dynamics of the PEO and PMMA in their blend matrix strongly depends on the composition of the polymers in the blend [3, 4, 6, 7, 9]. For improving the performance of the PEO/PMMA blend based SPEs, various inorganic nanofillers have also been dispersed in these ion-dipolar coordinated materials which result the nanocomposite solid polymer electrolytes (NSPEs) with promising properties [10–13, 20, 22, 23]. The electrochemical performance of such NSPEs depends on their amorphous phase, the polymer chain segmental dynamics, the available number of favorable ion conductive paths, and transient-type ion-polymer-nanofiller interactions [10, 13, 20, 22].

Besides the use of PEO/PMMA blends in the SPEs and NSPEs, this flexible blend matrix is highly interesting from the dielectric and electrical insulation point of view, and therefore there is an intense need of in-depth characterization of the dielectric and electrical properties of PEO/PMMA blend matrix dispersed with different nanofillers in order to understand the physics of such hybrid nanocomposite materials for confirmation of their technological applications [5, 6]. The synthetic polar and non-polar polymers are frequently used directly or indirectly, in almost all the areas of materials research because of their wide range of properties and design flexibility. However, for tailoring the useful properties of polymer matrices according to the technological requirements, various kinds of organic and inorganic nanomaterials have been used so far as filler for the development of multifunctional properties bearing polymer nanocomposite (PNC) materials [24–27]. It has already been established that the interfacial electrostatic interactions exhibited between the nanofiller and the functional group/s of the polymer chain greatly modify the structural, thermal, mechanical, permeable, environment/corrosion

resistance, flammability, optical, dielectric, and electrical properties of the PNC materials [25, 28–36]. These hybrid materials comprise most of the important technological properties of the flexible and lightweight polymer matrix and also the rigid inorganic nanofiller due to which they are recognized as multifunctional advanced polymeric nanodielectrics (PNDs) for their potential applications in the fabrication of high-performance flexible electrical and electronic devices [23, 24, 31, 33, 35–37]. Recently, authors have prepared and characterized numerous PND materials based on various polymer matrices and the polymer blend matrices, including the PEO and PEO/PMMA blend, dispersed with a variety of inorganic nanofillers in order to explore their technological applications, mainly related to the dielectric permittivity and electrical conductivity properties [5, 6, 32, 33, 37–45].

Among the ceramic nanomaterials, the alumina (Al_2O_3) nanopowder is cost-effective and bears highly promising thermomechanical properties [46]. Further, it is a transition ceramic material with a variety of meta-stable structural phases each having a different degree of crystallinity and the thermomechanical properties [47, 48]. Because of these facts, the Al_2O_3 nanopowder is largely used as an inorganic nanofiller for the preparation of various PNC materials [31, 37, 44, 45, 49–54] and also the novel NSPEs [10, 22, 23, 55–59].

Our survey of the literature reveals that the PEO/PMMA blend matrix incorporated with Al_2O_3 nanoparticles has not been studied for its dielectric and electrical properties so far. To fill this knowledge gap, the aims of the present work are: firstly, to prepare different concentrations Al_2O_3 nanoparticles filled partially miscible PEO/PMMA blend matrix (50/50 wt%)-based PNCs, and to characterize them by employing various advanced techniques in order to confirm the impact of Al_2O_3 mainly on the structural and dielectric properties of the blend matrix; and secondly, to compare the experimental results of PEO/PMMA- x wt% Al_2O_3 films with the literature values of several other PNC films having different polymer matrices and the various inorganic nanofillers in order to confirm the impact of interfacial effect on the dielectric and electrical properties of various PND materials; and finally, to explore in depth the useful properties of these hybrid nanocomposite polymeric materials in regard to their potential candidature in preparation of NSPEs, and also as PNDs for flexible electronics.

2 Experimental details

2.1 Materials and preparation of PNC films

For the preparation of PNC films, PEO powder of average molecular weight 600 kg mol^{-1} (CAS 25322-68-3), PMMA powder of average molecular weight 350 kg mol^{-1} (CAS 9011-14-7), and Al_2O_3 powder of particles sizes less than

50 nm (CAS 1344-28-1) were procured from Sigma-Aldrich, USA. Acetonitrile and tetrahydrofuran used as solvents for the PEO and PMMA, respectively, were received from Loba Chemie, India.

The solution-cast method was used for the preparation of PNC films consisted of PEO/PMMA blend matrix (50/50 wt%) incorporated with x wt% Al_2O_3 ($x=0, 1, 3,$ and 5 wt% amounts of Al_2O_3 with respect to the weight of PEO/PMMA blend). Initially, equal weight amounts of PEO and PMMA were dissolved in acetonitrile and tetrahydrofuran, respectively, and the same were mixed to get the polymer blend solution. The required amount of Al_2O_3 nanopowder for x wt% concentration was first dispersed into acetonitrile under vigorous magnetic stirring and then it was mixed slowly with the previously prepared polymer blend solution. This Al_2O_3 nanoparticle dispersed polymeric solution was further stirred continuously using magnetic stirrer until the homogeneous solution turns highly viscous. Subsequently, the viscous solution was cast on to Teflon petri dish and after evaporation of solvent at room temperature, the free-standing PNC film was obtained. The same steps were followed for the preparation of PNC films of different Al_2O_3

concentrations. The thicknesses of PEO/PMMA- x wt% Al_2O_3 films for x values 0, 1, 3, and 5 were 0.21, 0.20, 0.20, and 0.25 mm, respectively. Prior to characterization, the solvent traces were removed by vacuum drying of the PNC films at 40 °C for 24 h.

2.2 Characterization techniques

The Carl ZEISS EVO 18 SEM was used for the morphological study of the PNC films. PANalytical X'pert Pro MPD diffractometer of copper- K_α radiation was employed for recording the X-ray diffraction (XRD) patterns to examine the crystalline phases of the films and their degree of crystallinity, whereas an Agilent FTIR spectrometer (Cary 630) was used for recording the FTIR spectra in the wavenumber range from 400 to 4000 cm^{-1} to confirm the polymer-polymer and polymer-nanoparticle interactions in these PNC materials. Agilent technologies precision LCR meter (4284A) equipped with a solid dielectric test fixture (16451B) was used for the dielectric and electrical characterization of the PNC films over the frequency range from 20 Hz to 1 MHz.

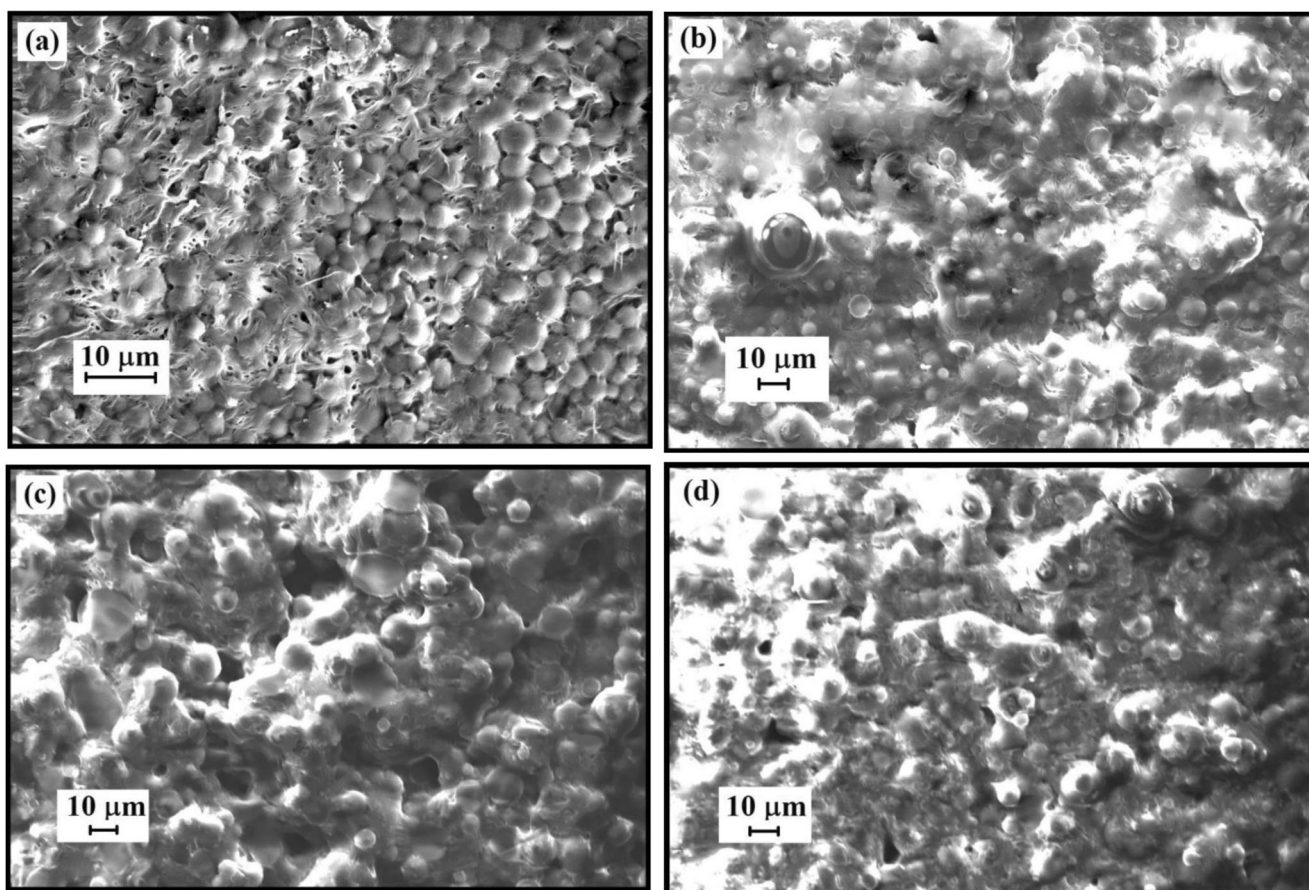


Fig. 1 SEM images of (PEO/PMMA)- x wt% Al_2O_3 films for **a** $x=0$, **b** $x=1$, **c** $x=3$, and **d** $x=5$

3 Results and discussion

3.1 SEM micrographs and morphological analysis

Figure 1 depicts the SEM micrographs of (PEO/PMMA)- x wt% Al_2O_3 films. It can be noted from Fig. 1a that the surface of pristine PEO/PMMA blend film is rough, porous, and there are homogeneously distributed microsize PEO spherulites. The presence of PEO spherulites reveals that the 50/50 wt% blend of PEO and PMMA is partially miscible. It is because of the fact that for the highly compatible and miscible blend of PEO/PMMA, almost all the PEO spherulites which represent the PEO crystallinity must vanish owing to the stretching of PEO chain, when PMMA forms the molecular interactions with PEO quite uniformly over the entire structure of the blend, as reported earlier for the PMMA-rich PEO/PMMA blend [1, 3, 6]. Further, it is found that the addition of merely 1 wt% Al_2O_3 in the PEO/PMMA blend microstructures results in significantly different morphology of the PNC film (Fig. 1b) as compared to that of the PEO/PMMA blend film (Fig. 1a). It can be seen that the number of PEO spherulites per unit area decreases by collapsing together resulting in a spongy morphology with the formation of bigger size pores. This finding confirms that the polymer-nanoparticle interactions bridge the PEO and PMMA more strongly with their chains stretching, owing to which the PEO spherulites decrease. The sizes of PEO spherulites, their density and distribution, and the pore sizes change with the further increase of Al_2O_3 amounting up to 5 wt% in the PEO/PMMA blend (Fig. 1c, d). These SEM images also reveal that the Al_2O_3 nanoparticles are quite homogeneously dispersed in the PEO/PMMA blend matrix and the nanofiller aggregates are insignificant with the loading of Al_2O_3 up to 5 wt%. The observed changes in the microstructures of the blend polymer composite on Al_2O_3 addition are increase of homogeneity, amorphous phase, and porosity which confirms the hybrid polymer composite as a potential candidate for the base matrix in the preparation of novel NSPE materials as used earlier [10, 23].

3.2 XRD patterns and structural analysis

Figure 2a shows that the XRD pattern of Al_2O_3 nanoparticles over the Bragg's angle range 10–80° has several low intensity diffraction peaks which are in good agreement of the peak position and intensities of the γ -phase Al_2O_3 diffractogram [37, 47, 48]. The XRD patterns of (PEO/PMMA)- x wt% Al_2O_3 films are shown in Fig. 2b. It was earlier explored that the semicrystalline PEO film exhibits the highly intense and sharp characteristic diffraction peaks at 19.22° and 23.41° which are associated with (120) and concerted (112),(032) reflection planes of the PEO crystallites, respectively [37]. Therefore, the diffraction peaks observed at 19.54° and 23.66° in the XRD

pattern of pristine PEO/PMMA blend film (i.e., $x = 0$) represent the presence of PEO crystalline phase in the blend. It can be noted from the figure that the addition of 1 wt% Al_2O_3 nanoparticles in the PEO/PMMA blend

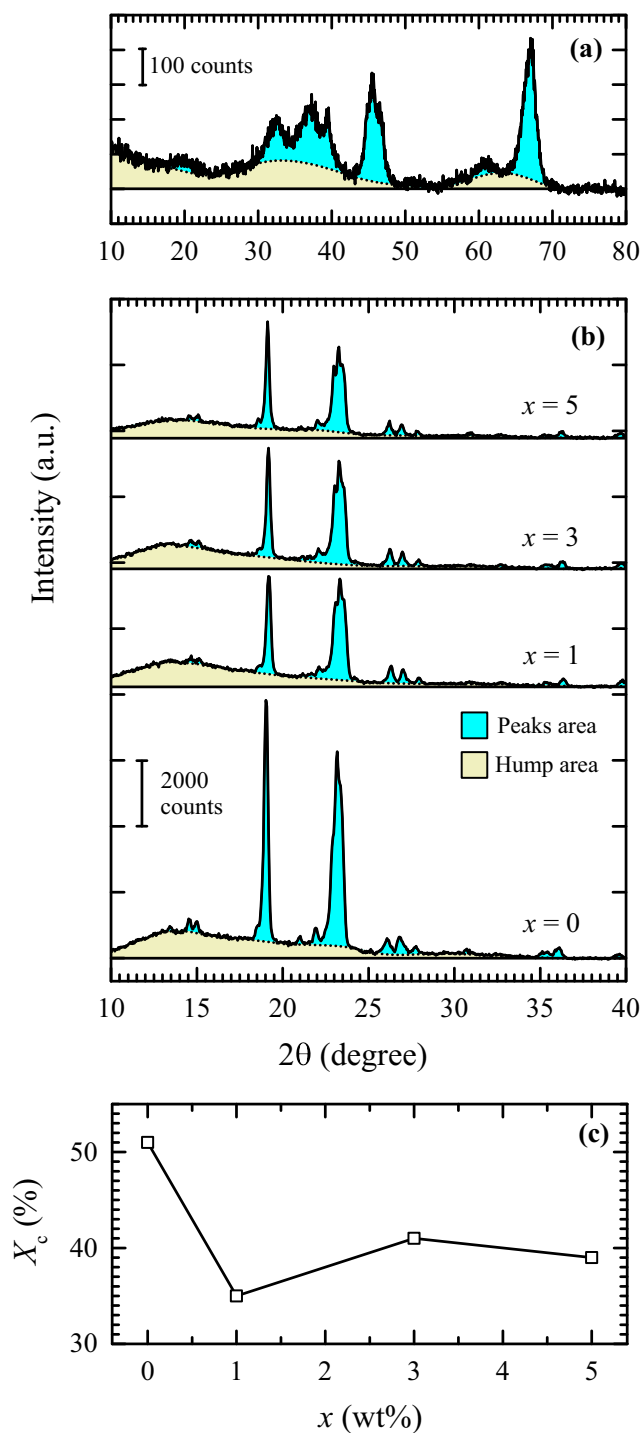


Fig. 2 The XRD patterns of **a** Al_2O_3 nanopowder; **b** (PEO/PMMA)- x wt% Al_2O_3 films of x values 0, 1, 3, and 5 with highlighted areas of the crystalline peaks and the hump; and **c** percentage degree of crystallinity versus Al_2O_3 concentration plot for the PNC films

reduces the diffraction peak intensities by about half which confirms that the polymer-nanoparticle interactions break some domains of PEO crystallites and therefore, the crystalline phase of the composite decreases. From Fig. 2b, it is noted that on further increase of Al_2O_3 nanoparticle concentration up to 5 wt% in the PEO/PMMA blend matrix, there is a little variation in the intensities of the diffraction peaks which also infers minor alteration in the behavior of polymer-nanoparticle interactions.

The percentage degree of crystallinity X_c (%) of these PNC materials and their constituents were determined using the relation $X_c (\%) = (A_P / (A_P + A_H)) \times 100$, where A_P is the sum of the areas of all the crystalline peaks and A_H is the area of the hump under the XRD pattern [20]. The A_P and A_H values of these materials were calculated from their XRD patterns by using the OriginPro® version-8 software. In Fig. 2a and b, the A_P and A_H portions are highlighted by shaded portions between the XRD patterns and the baselines for the Al_2O_3 powder and also for the (PEO/PMMA)- x wt% Al_2O_3 films. Figure 2c depicts the variation of X_c (%) with the Al_2O_3 concentration x (wt%) of the PNC films. It is found that the X_c value of 1 wt% Al_2O_3 containing PNC film is low by 16% as compared to that of the PEO/PMMA blend film. On further increase of Al_2O_3 concentration, the X_c values of these PNC films slightly increase and is about 40% for both the 3 and 5 wt% Al_2O_3 dispersed PNC films, yet significantly lower

than that of the pristine blend film ($X_c = 51\%$). These results confirm that the Al_2O_3 nanoparticles added PEO/PMMA blend-based composite materials are more amorphous as compared to the amorphous phase of the pristine blend which is consistent with their SEM results.

3.3 FTIR spectra and polymer-nanofiller interaction

Figure 3 presents the FTIR spectra of (PEO/PMMA)- x wt% Al_2O_3 films over the wavenumber range from 400 to 4000 cm^{-1} . The wavenumbers of various absorption bands of the PEO/PMMA blend film are marked in the figure which are attributed to the characteristic vibrational modes corresponding to the twisting, wagging, bending, scissoring, stretching, and rocking of the various structural groups/parts of the PEO and PMMA monomer units as defined in the literature [6, 15, 19, 22, 60]. A close look on the FTIR spectra of these materials reveals that the spectrum of each PNC film fairly resembles with that of the pristine PEO/PMMA blend film, but the intensities of several peaks vary significantly with the increase of Al_2O_3 concentration without any observable shift in any of the peak positions. The variations in the peak intensities clearly imply the interaction of Al_2O_3 nanoparticles with the functional groups of PEO and PMMA chains in their blend matrix. Further, the comparative results of FTIR, XRD, and SEM of these materials confirm that the nanocomposites

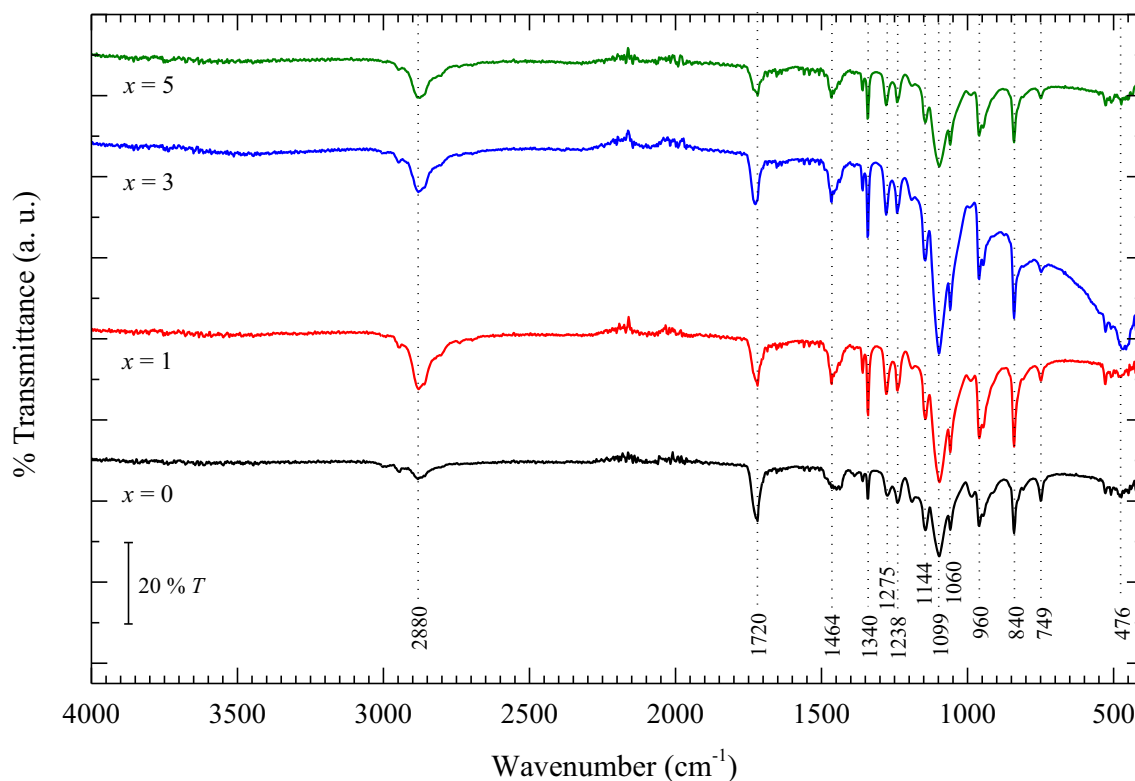


Fig. 3 FTIR spectra of (PEO/PMMA)- x wt% Al_2O_3 films for x values 0, 1, 3, and 5. Wavenumber values of various vibrational bands of the pristine PEO/PMMA blend are marked in the figure

are appropriately formed due to homogeneous dispersion of Al₂O₃ nanoparticles in the PEO/PMMA blend and also their large-range interactions with the microstructures of the blended polymers.

3.4 Complex dielectric permittivity

Figure 4 depicts the real part ϵ' of complex permittivity and the dielectric loss tangent $\tan\delta$ (defined by ϵ''/ϵ' where ϵ'' is the loss part of complex permittivity) spectra of (PEO/PMMA)- x wt% Al₂O₃ films at 30 °C, and also with temperature variation in the range 30–60 °C for the (PEO/PMMA)-3 wt% Al₂O₃ film as a representative sample. Figure 4a shows that the ϵ' values of these materials at fixed temperature (30 °C) are almost frequency independent in the radio frequency range (RF-region) (i.e., from 20 kHz to 1 MHz), whereas the ϵ' increases significantly with the decrease of frequency from 20 kHz to 20 Hz in the audio frequency range (AF-region). The enhancement of ϵ' values in the low frequency domain for these PNC materials is due to interfacial polarization (IP)

effect which is also known as Maxwell-Wagner-Sillars (MWS) dielectric polarization process as noted in most of the composite materials [31–33, 37–44, 49, 61–66]. Maxwell and later on Wagner and Sillars demonstrated the dielectric polarization theory of composite materials in the low-frequency region and according to this theory, under the slowly varying electric field, the charge accumulation, electric field redistribution, enhanced polarization, and boosted dielectric response will occur at interfaces between the different constituents that possess distinct permittivity in a blend or hybrid composite material as also reported recently [49, 65, 66]. Further, in addition to these changes, there is also suppression of leakage conductance and loss due to blocking of charge transportation by the interfaces in such hybrid dielectric materials under the influence of low-frequency electric field [65].

It can be noted from Fig. 4a that for these PNC films, at a fixed frequency, the values of ϵ' anomalously change with the increase of Al₂O₃ concentration in the PEO/PMMA blend matrix which reflects a huge variation in the dipolar

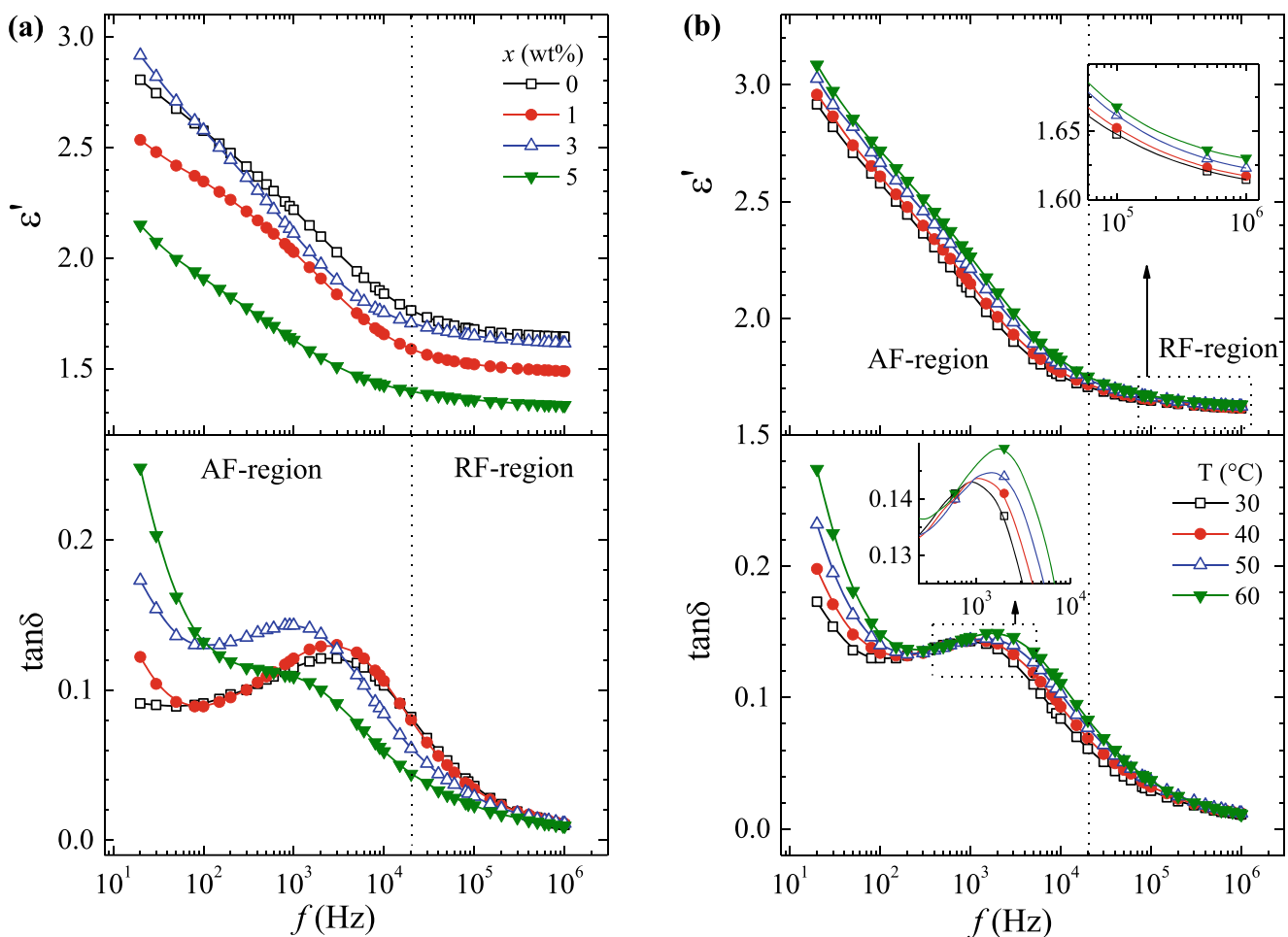


Fig. 4 The spectra of real part ϵ' of the complex dielectric permittivity and the loss tangent $\tan\delta$ of **a** (PEO/PMMA)- x wt% Al₂O₃ films for x values 0, 1, 3, and 5 at 30 °C, and **b** (PEO/PMMA)-3 wt% Al₂O₃ film at

temperatures 30, 40, 50, and 60 °C. The insets show the enlarged view of ϵ' at high frequencies and the peaks of the $\tan\delta$ plots

ordering of the polymer structures in the films. The ε' values of these PNC materials at radio frequencies are found in the range 1.25 to 1.75 which are significantly low, but at audio frequencies, the ε' increases and displays the values in the range 2 to 3 at 20 Hz. These ε' values categorize the studied PNC materials as low-dielectric constant nanodielectrics. The $\tan\delta$ spectra of these materials presented in the lower layer of the figure exhibit relaxation peak below 10 kHz which is attributed to cooperative chain segmental relaxation process of the PEO and PMMA molecules in their complex structures [6, 42]. The values of segmental dynamic process relaxation time τ_s were determined using the $\tan\delta$ peak frequency f_p values in the relation $\tau_s = 1/\omega_p$, where $\omega_p = 2\pi f_p$, and it is observed that these τ_s values for the PNC materials unsystematically increase with the enhancement of nanofiller concentration which is discussed in detail in the later section.

In order to examine the temperature-dependent dielectric behavior of these PNC materials, the (PEO/PMMA)–3 wt% Al_2O_3 film was considered as an appropriate material due to its relatively high dielectric permittivity value, and therefore it

was studied with the temperature variation as a representative sample. Figure 4b shows that the ε' of (PEO/PMMA)–3 wt% Al_2O_3 film has a little increase with the increase of its temperature from 30 to 60 °C, and the $\tan\delta$ peak of this film has a gradual shift towards higher frequency side with a small enhancement in its magnitude with the temperature increase. These results confirm that both the dielectric behavior and the structural dynamics of the PNC material are thermally activated processes, i.e., these values enhance with the increase of temperature which is owing to the enhancement of free volume in the material.

In order to understand the effect of nanofiller concentration x (wt%) and the temperature T (°C) on the complex permittivity behavior of these PNC materials, the ε' and ε'' values as a function of x (wt%) for the (PEO/PMMA)– x wt% Al_2O_3 films and also as a function of T (°C) for the (PEO/PMMA)–3 wt% Al_2O_3 film at some selective frequencies are depicted in Fig. 5. It can be noted from Fig. 5a that the ε' values anomalously vary with the increase of Al_2O_3 concentration in the PEO/PMMA blend matrix at all the fixed frequencies which reveal that

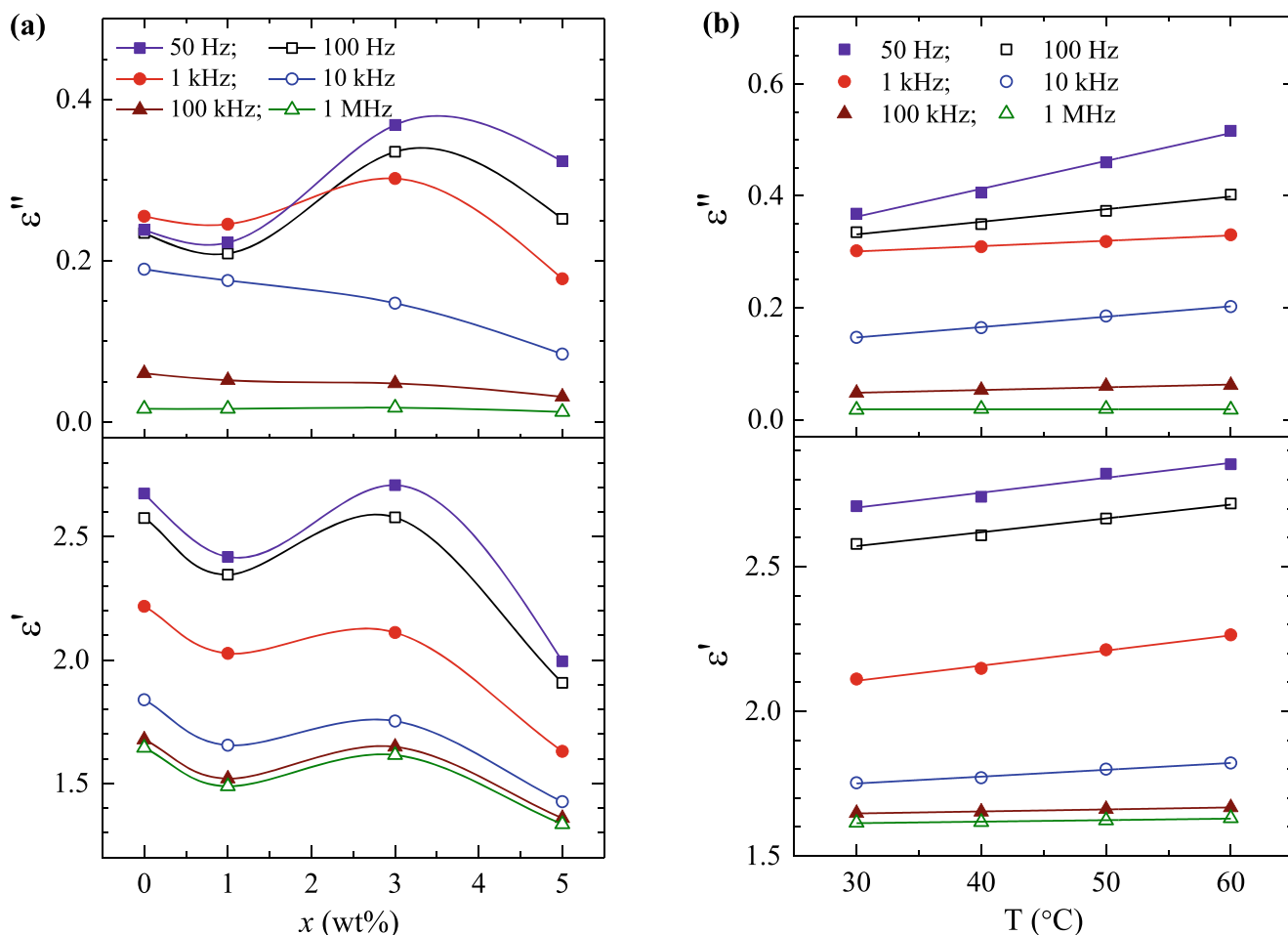


Fig. 5 Dependence of ε' and ε'' values on **a** x (wt%) concentration of Al_2O_3 nanofiller for (PEO/PMMA)– x wt% Al_2O_3 films for x values 0, 1, 3, and 5, at 30 °C, and **b** temperatures T (°C) for (PEO/PMMA)–3 wt% Al_2O_3 film, at several fixed frequencies

the polymer-nanoparticle interactions depend on the filler concentration and alter the polymer dipolar ordering unsystematically. Further, Fig. 5a shows that the ϵ'' values of these PNC films vary anomalously with the increase of nanofiller concentration at 50 Hz, 100 Hz, and 1 kHz, whereas at 10 kHz and 100 kHz, they gradually decrease. Further, at 1 MHz, the ϵ'' values are almost independent of nanofiller concentration and these values are relatively very low. Figure 5b shows that at all the fixed frequencies, the ϵ' and ϵ'' linearly increase with the increase of temperature of the (PEO/PMMA)–3 wt% Al_2O_3 film but the rate of increase gradually enhances as the frequency of applied electric field decreases. Further, at radio frequencies, the relative increase in ϵ' and ϵ'' values with the increase of temperature is very small, and therefore this 3 wt% Al_2O_3 containing PNC material can be used as temperature independent nanodielectric over the range 30–60 °C and also as low-dielectric permittivity material at radio frequencies.

3.5 Electric modulus spectra

The electrical relaxation processes associated with the structural and charge dynamics in a hybrid composite material can be analyzed in depth by deriving its electric modulus spectrum from the complex permittivity spectrum [33, 38, 41, 67–70]. The obtained spectra of the real M' and imaginary M'' parts of the complex electric modulus of (PEO/PMMA)– x wt% Al_2O_3 films at 30 °C, and also with the temperature variation in the range 30–60 °C for the (PEO/PMMA)–3 wt% Al_2O_3 film are depicted in Fig. 6. The M' values nonlinearly increase with the increase of frequency in the AF-region, whereas over the RF-region, the M' values are almost frequency independent for these materials which is expected from the shape of their complex dielectric permittivity spectra because these functions are mutually reciprocal as reported in the literature [33, 70]. The M'' spectra of the PNC films (Fig. 6a) exhibit more noticeable relaxation peak in the intermediate frequency range as compared to that observed in their $\tan\delta$ spectra (Fig. 4a). Similar to

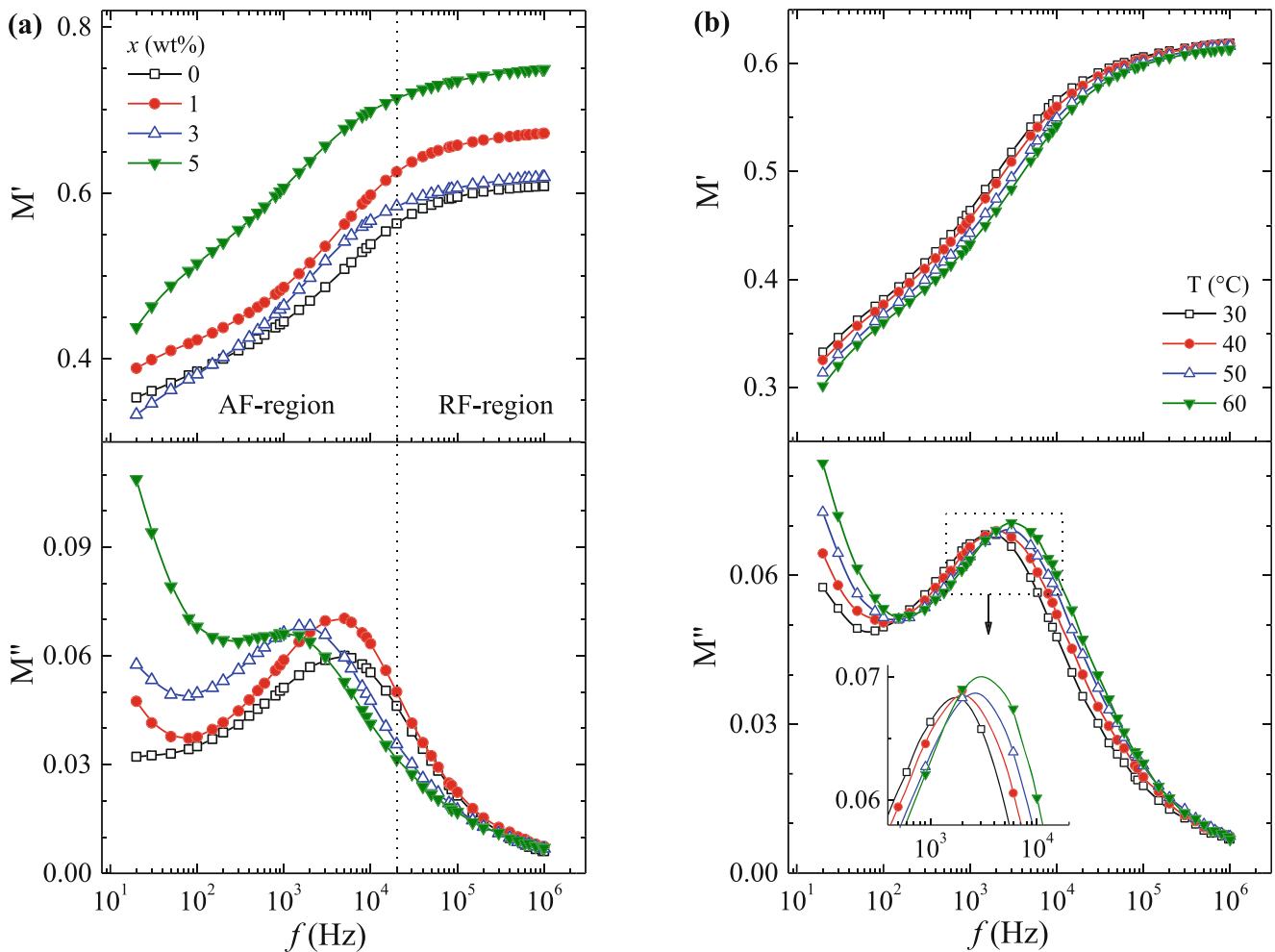


Fig. 6 Frequency-dependent real part M' and loss part M'' of complex electric modulus of **a** (PEO/PMMA)– x wt% Al_2O_3 films for x values 0, 1, 3, and 5 at 30 °C, and **b** (PEO/PMMA)–3 wt% Al_2O_3 film at temperatures

30, 40, 50, and 60 °C. The inset shows the enlarged view of peaks exhibited in the M'' plot with temperature variation

the peaks in $\tan\delta$ spectra, the M'' peak positions on the frequency scale also vary unevenly with the increase of Al_2O_3 concentration in the PEO/PMMA blend matrix, whereas a gradual enhancement and shift towards higher frequency side can be noticed from the inset of Fig. 6b as the temperature of the PNC film increases. The values of modulus relaxation time τ_M for these PNC materials were determined by taking the M'' peaks frequency $f_{p(M)}$ values from their M'' spectra and using the relation $\tau_M = 1/2\pi f_{p(M)}$.

The τ_M values along with the τ_s values (determined from the $\tan\delta$ spectra as stated in the previous Section 3.4) as a function of x (wt%) concentration of Al_2O_3 for these PNC materials are plotted in Fig. 7a. Further, the logarithmic τ_s and τ_M versus $1000/T$ plots for the 3 wt% Al_2O_3 containing PNC film are depicted in Fig. 7b. It can be seen from Fig. 7a that the τ_s is always greater than the corresponding τ_M at all the concentrations of Al_2O_3 in the PNC films. This relative characteristic behavior of these relaxation times (i.e., $\tau_s > \tau_M$) has also been noted in several PNC materials [6, 37, 38, 42]. Furthermore, it can be noted from Fig. 7b that the temperature-dependent relaxation times of the PNC film obey the Arrhenius behavior. The activation energy values determined

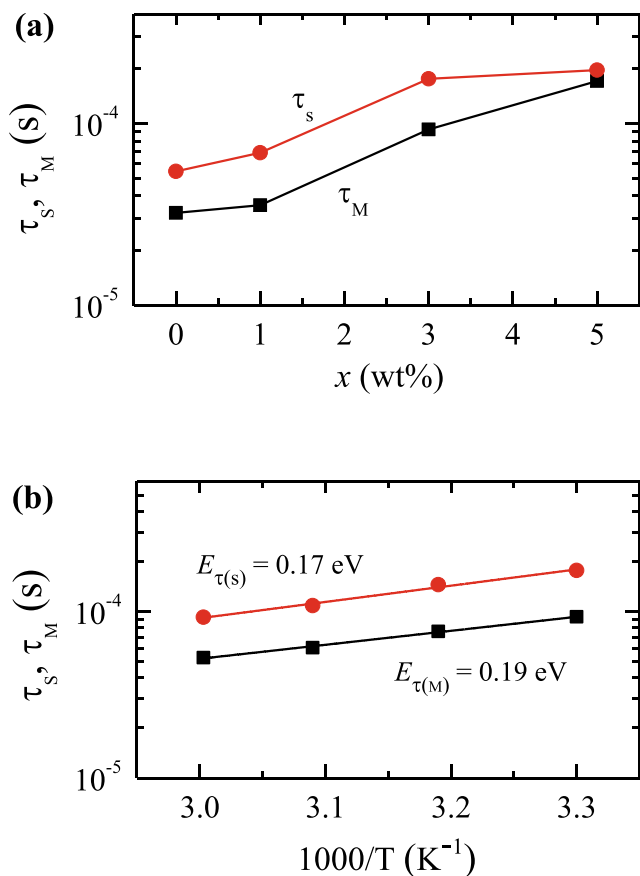


Fig. 7 **a** Al_2O_3 concentration-dependent relaxation times τ_s and τ_M of (PEO/PMMA)- x wt% Al_2O_3 films for x values 0, 1, 3, and 5 at 30 °C, and **b** the Arrhenius plots of the relaxation times τ_s and τ_M of (PEO/PMMA)-3 wt% Al_2O_3 film

from the slopes of the Arrhenius plots are found low ($E_{\tau(s)} = 0.17$ eV and $E_{\tau(M)} = 0.19$ eV) confirming that the potential barrier for the relaxing polymer chain segments and the transporting charges is significantly low. Such low potential barrier of these PNC materials also favors their suitability as base matrices for the preparation of NSPEs with doping of alkali metal salts as investigated earlier [10, 22].

3.6 Conductivity and impedance spectra

The spectra of alternating current (ac) electrical conductivity (σ' and σ'') and complex impedance (Z' and Z'') of the (PEO/PMMA)- x wt% Al_2O_3 films are reported in Fig. 8. These spectra are significantly important in regard to the use of such materials as nanodielectrics in the design and development of electronic devices, namely capacitors, antennas, organic field effect transistors, and also as coating material for electromagnetic interference shielding because the performance of such devices is strongly determined by the conductivities of these dielectric materials [29, 31, 65]. Figure 8 explains that the electrical conductivity and impedance values of these PNC films slightly changes with the variation of Al_2O_3 nanofiller concentration up to 5 wt%, whereas the effect of temperature variation on these properties of a PNC film is found insignificant over the range 30–60 °C. Further, the σ' values at 20 Hz are of the order of 10^{-12} S/cm which confirms that these nanodielectric materials can be used as prominent electrical insulators at the low-frequency electric field and also as the direct current (dc) electric field-activated microelectronic devices. The high impedance values at low frequencies too favors their high electrical insulation behavior which significantly improves for 5 wt% Al_2O_3 containing PEO/PMMA blend-based PNC film.

3.7 Comparison of dielectric properties with other PNC materials

The literature values of the real part ϵ' of complex dielectric permittivity at 100 Hz, 1 kHz, and 1 MHz frequencies, dc electrical conductivity σ_{dc} and relaxation time τ_s of the polymer chain segmental dynamics without and with inorganic oxide nanofiller-based films, at room temperature, are listed in Table 1 and these are compared with the data of the PNC materials studied in this work. The dielectric parameters included in Table 1 are of the host matrices of PEO and its 50/50 wt% blend with PMMA, poly(vinyl pyrrolidone) (PVP), and poly(vinyl alcohol) (PVA) dispersed with 5 wt% oxide nanofillers, namely alumina (Al_2O_3), silica (SiO_2), zinc oxide (ZnO), and tin oxide (SnO_2). The ϵ' and σ_{dc} values of PVA and PVA/PVP blend-based PNCs and also polyimide (PI) and 5 wt% Al_2O_3 containing PI-based nanodielectric have also been given in Table 1 although these materials do not exhibit relaxation process in the frequency range 20 Hz to 1 MHz, at room

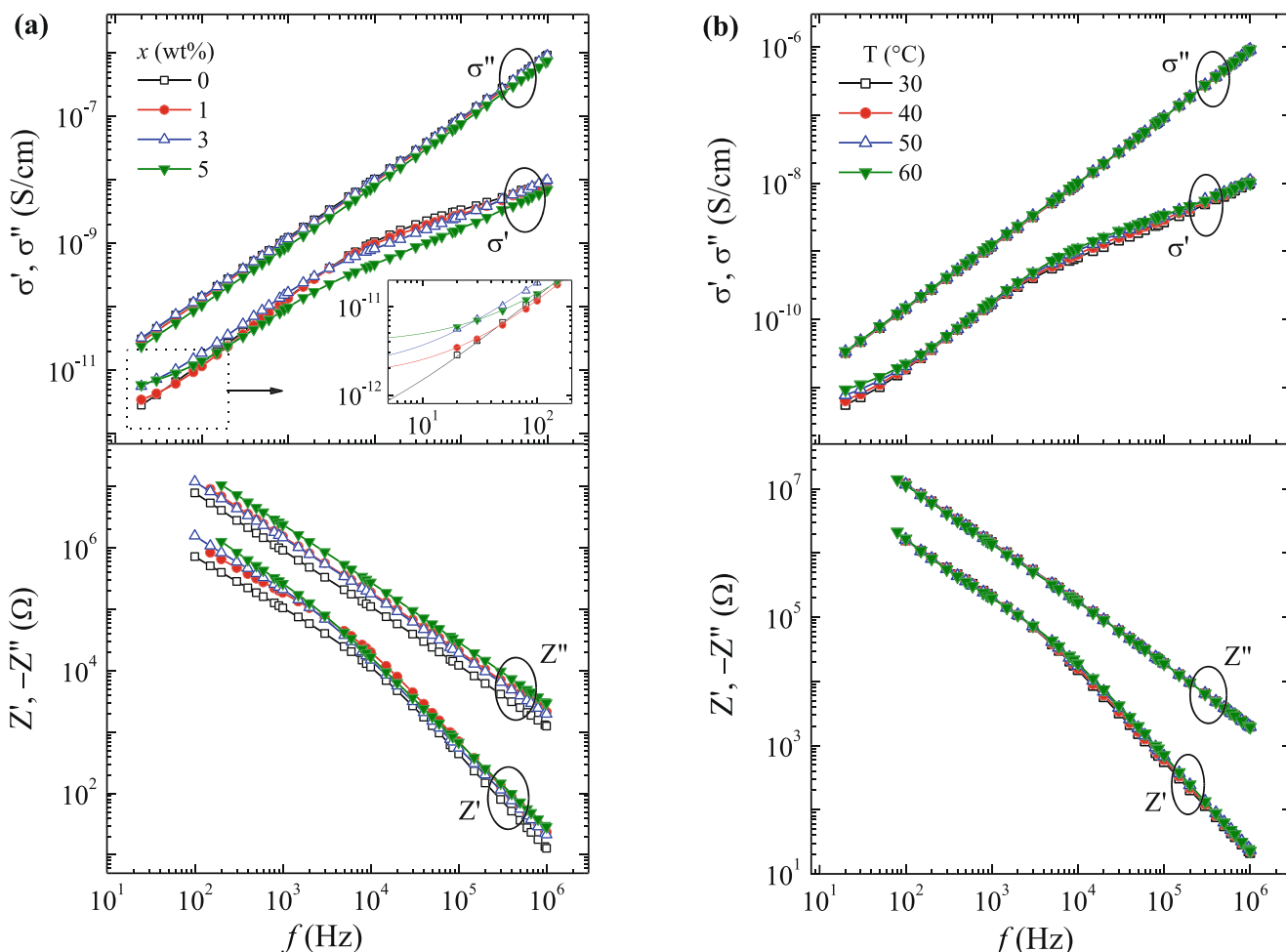


Fig. 8 Frequency-dependent real part σ' and loss part σ'' of the complex ac electrical conductivity, and the real part Z' and reactive part Z'' of the complex impedance of **a** (PEO/PMMA)- x wt% Al_2O_3 films for x values

0, 1, 3, and 5 at 30 °C, and **b** (PEO/PMMA)-3 wt% Al_2O_3 film at temperatures 30, 40, 50, and 60 °C. The inset shows the power law fit of the σ' data at low frequencies

temperature. The ϵ' values of the nanofillers Al_2O_3 , SiO_2 , ZnO , and SnO_2 are 9.7, 3.8, 10.26, and 34.5, respectively, at 1 MHz and 27 °C [22, 53]. Further, the particle sizes of these Al_2O_3 , SiO_2 , ZnO , and SnO_2 nanofillers used for the preparation of PNC films are less than 50, 15, 100, and 100 nm, respectively, as given in the literature [22]. The films of polymers, polymer blends, and their PNCs given in Table 1 were prepared by the solution casting using appropriate solvents, except the PEO-5 wt% SiO_2 and PI-5 wt% Al_2O_3 films which were prepared by melt-mixing and via the in situ polymerization, respectively, as reported in the literature (references given in Table 1). Further, the PEO/PMMA-5 wt% SiO_2 film was prepared by solution-cast followed by melt pressing in order to get its smooth surfaces. Therefore, the effect of film preparation methods has also been considered during the analysis of comparative variation in dielectric parameters of these materials along with the effects of polymer structures, various polymer blends, and oxide nanofillers. In Table 1, the dielectric parameters of these PNC materials for 5 wt% concentration of the nanofillers are reported for the comparison, although the

dielectric and electrical data for the different concentrations of these nanofillers over the wide frequency range are available in the respective references mentioned in the table.

From Table 1, it can be noted that the ϵ' values of solution-cast PEO-based PNC films [37, 38], at fixed frequencies, are lower than that of the pristine PEO film [38] except at 1 MHz for the PEO-5 wt% SiO_2 film which was prepared by melt-pressing method [40]. The lowering of ϵ' values of these PNC films clearly reflects that all these nanofillers destruct the dipolar ordering of PEO structures which also vary with the type of oxide nanofiller used in these films. Results clearly reveal that the nanoparticle sizes and their dielectric constant significantly influence the ϵ' values of these nanofillers incorporated PEO-based PNC films. It is also noted that the presence of inorganic nanofillers reduces the electrical conductivity of these PNC films and also hinders the PEO chain segmental dynamics as revealed from the relatively many times increased τ_s values.

The film of PEO blended with PMMA, in equal weight amounts, exhibits a huge lowering of the ϵ' and σ_{dc} values, whereas its τ_s value enhances largely as compared to that of

Table 1 Values of the real part ϵ' of complex dielectric permittivity (at 100 Hz, 1 kHz, and 1 MHz), dc electrical conductivity σ_{dc} , and chain segmental dynamics relaxation time τ_s of the polymers, polymers blends (50/50 wt%), and polymer nanocomposite (PNC) films at room temperature (~27–30 °C)

Polymer/PNC films	ϵ'			σ_{dc} ($\times 10^{-12}$ S/cm)	τ_s (μ s)	References
	100 Hz	1 kHz	1 MHz			
PEO	9.93	7.30	2.61	38.8	8.7	[38]
PEO–5 wt% Al_2O_3	4.27	3.17	1.95	10.5	94.0	[37]
PEO–5 wt% ZnO	4.80	4.21	2.2	9.0	20.0	[38]
PEO–5 wt% SiO_2	9.80	6.59	3.12	0.8	78.8	[40]
PEO/PMMA	2.58	2.23	1.64	2.0	54.5	Present work
PEO/PMMA–5 wt% Al_2O_3	1.91	1.63	1.33	6.0	196.4	Present work
PEO/PMMA–5 wt% SiO_2	6.39	3.88	2.59	3.6	780.6	[6]
PEO/PMMA–5 wt% SnO_2	12.76	8.72	2.33	39.6	9.30	[42]
PEO/PVP	2.60	2.19	1.91	1.3	1212.0	[71]
PEO/PVP–5 wt% ZnO	3.84	3.03	2.43	3.5	573.0	[71]
PEO/PVP–5 wt% SiO_2	2.86	2.31	1.98	1.3	375.6	[32]
PEO/PVA	5.11	4.52	2.80	13.3	11.0	[45]
PEO/PVA–5 wt% Al_2O_3	6.37	5.16	2.90	41.9	4.5	[45]
PEO/PVA–5 wt% ZnO	5.80	4.55	2.75	15.9	4.0	[41]
PEO/PVA–5 wt% SiO_2	5.20	4.6	2.8	7.6	9.7	[72]
PVA/PVP	3.94	3.47	2.83	2.7	–	[44]
PVA/PVP–5 wt% Al_2O_3	3.50	3.33	2.85	0.29	–	[44]
PVA/PVP–5 wt% ZnO	5.92	4.56	3.48	6.8	–	[33]
PVA/PVP–5 wt% SiO_2	3.97	3.54	2.87	2.3	–	[39]
PVA	4.64	4.33	3.41	0.26	–	[54]
PVA–5 wt% Al_2O_3	6.28	5.63	4.25	0.32	–	[54]
PVA–5 wt% ZnO	6.60	5.64	3.82	10.1	–	[73]
PVA–5 wt% SiO_2	3.42	3.23	2.74	1.1	–	[74]
PI	3.35	3.33	3.28	0.08	–	[49]
PI–5 wt% Al_2O_3	3.62	3.58	3.51	0.15	–	[49]

the pristine PEO film. These parameters confirm that there is less dipolar ordering and relatively slow charge conduction process in this blend, and also more hindrance to the cooperative chain segmental dynamics of the polymers which is expected owing to bulky repeat unit of PMMA as compared to that of the PEO. From Table 1, it can be seen that the addition of Al_2O_3 in the PEO/PMMA blend reduces the ϵ' values while the SiO_2 - and SnO_2 -added PNC films have a large enhancement in their ϵ' values [6, 42]. The σ_{dc} of all these PNC films are high as compared to that of the pristine PEO/PMMA blend which confirms that the charge conduction process enhances in the presence of these oxide nanofillers. Further, the τ_s values of these PNC materials reveal that the cooperative chain segmental dynamics of the PEO/PMMA is greatly hindered by the Al_2O_3 and SiO_2 nanoparticles, but it is significantly promoted by the SnO_2 nanoparticles which may be due to its high dielectric constant.

From Table 1, one can see that the blending of PEO with PVP also lowers the ϵ' values of PEO which is in agreement to that of the PEO/PMMA blend. The σ_{dc} value of PEO/PVP blend is very low and the τ_s value is extremely high as compared to that of the pristine PEO film which is because of the bulky size of the

repeat unit of PVP. When ZnO and SiO_2 nanoparticles were added in the PEO/PVP blend matrix, then the PNC films of these materials exhibit a slight increase in ϵ' values, a small change in σ_{dc} , and a large decrease in τ_s values [32, 71]. The decrease of τ_s reveals that the presence of ZnO and SiO_2 accelerates the cooperative chain segmental dynamics in the PEO/PVP blend. In comparison to the PEO/PMMA and PEO/PVP blends, the ϵ' values of PEO/PVA blend and its nanofiller dispersed PNC films are slightly high at all the frequencies [41, 45, 72]. Further, the σ_{dc} values for Al_2O_3 and ZnO nanoparticle-loaded PEO/PVA blend-based PNC films were enhanced, whereas it reduced for the SiO_2 nanoparticle-added PNC film as compared to that of the pristine PEO/PVA blend film. Interestingly, the τ_s value of PEO/PVA blend is much lower than that of the PEO/PMMA and PEO/PVP blend films, and also the addition of Al_2O_3 , ZnO, and SiO_2 nanoparticles accelerates the cooperative chain segmental dynamics of the PEO/PVA structures. The relative changes in the dielectric parameters of these blends and their PNC films in which PEO is one of the common constituents are expected because the pendant group of PVA chain monomer unit is much smaller as compared to that of the PMMA and PVP chain repeat units.

In case of PVA/PVP blend and its PNC films, it can be noted from Table 1 that there is also a variation in the ϵ' and σ_{dc} values with the type of oxide nanofiller loaded in this blend matrix [33, 39, 44]. Further, the ϵ' and σ_{dc} values of pristine PVA film and the Al_2O_3 , ZnO, and SiO_2 nanoparticles loaded its PNC films [54, 73, 74] also reveal that these dielectric parameters depend greatly on the inorganic nanofiller used in the preparation of these nanodielectric materials. The ϵ' values of pristine PI film are almost frequency independent, whereas the addition of 5 wt% Al_2O_3 slightly enhances its ϵ' and σ_{dc} values [49]. The films of PVA, PVA/PVP blend, and PI and also their PNCs do not exhibit the relaxation process over the frequency range 20 Hz to 1 MHz corresponding to the polymer chain segmental dynamics [33, 39, 44, 49, 54, 73, 74]. The dielectric and electrical parameters of the various PNC films listed in Table 1 and also in-depth exploration of their dependence on the polymers structures and the type of nanofillers are interesting in regard to choose a technologically required material, that could be used as flexible polymeric nanodielectric in the hybrid material-based electrical and electronic devices, including some biodegradable advanced multifunctional devices for next-generation flexible electronics [31, 33, 36, 75–79].

4 Conclusions

The morphological, structural, dielectric, and electrical behavior of $(\text{PEO}/\text{PMMA})-x$ wt% Al_2O_3 films having $x = 0, 1, 3,$ and 5 were reported. It is found that the dispersion of Al_2O_3 nanoparticles in the PEO/PMMA blend significantly modifies the size and shape of PEO spherulites in the PNC films which is due to the formation of polymer-nanoparticle interactions and simultaneous alteration of the PEO/PMMA blend polymer-polymer interactions. These materials are semicrystalline and their crystalline phase is because of the PEO spherulites, and the incorporation of Al_2O_3 reduces the degree of crystallinity. The dielectric permittivity of the PNC films is almost frequency independent over the radio frequency region, but it increases with the decrease of frequency in the audio frequency region which is due to the dominant contribution of interfacial polarization. Further, the dielectric permittivity of the PNC films anomalously varies with the increase of nanofiller concentration, whereas it has a linear increase with the increase of film temperature. In these materials, the cooperative chain segmental dynamics of the polymers decreases with the increase of nanofiller concentration as evident from the increase of dielectric relaxation time of this process. The relaxation time activation energy of the 3 wt% Al_2O_3 containing PNC film is found $E_r \sim 0.18$ eV confirming a significantly low potential barrier for the chain segmental dynamics. The RF-region real part of dielectric permittivity is less than 2 which categorizes these PNC films as low-

dielectric constant flexible nanodielectrics, whereas the AF-region dielectric permittivity of these materials is frequency tunable in the range of 1.5 to 3 and also depends on the nanofiller concentration. The low activation energy and reduced crystallinity also suggest the suitability of these PNC matrices as a potential candidate for the preparation of nanocomposite solid polymer electrolytes. The dielectric and electrical parameters of these polymeric nanodielectrics were also compared with that of the other PNC films based on different polar polymers and their blend films dispersed with Al_2O_3 , SiO_2 , ZnO, and SnO_2 nanoparticles, and the effect of various nanofillers on the dielectric permittivity, electrical conductivity, and the polymer chain segmental dynamics were recognized.

Acknowledgments One of the authors (PD) thanks the CSIR, New Delhi, for the award of a postdoctoral research associate fellowship.

Compliance with ethical standards

Conflict of interest The authors declare that they have no conflict of interest.

Publisher's note Springer Nature remains neutral with regard to jurisdictional claims in published maps and institutional affiliations.

References

- Liau WB, Chang CF (2000) Casting solvent effect on crystallization behavior and morphology of poly(ethylene oxide)/poly(methyl methacrylate). *J Appl Polym Sci* 76:1627–1636
- Sakai VG, Chen C, Maranas JK, Chowdhuri Z (2004) Effect of blending with poly(ethylene oxide) on the dynamics of poly(methyl methacrylate): a quasi-elastic neutron scattering approach. *Macromolecules* 37:9975–9983
- Ghelichi M, Qazvini NT, Jafari SA, Khonakdar HA, Farajollahi Y, Scheffler C (2013) Conformational, thermal and ionic conductivity behavior of PEO in PEO/PMMA miscible blend: investigating the effect of lithium salt. *J Appl Polym Sci* 129:1868–1874
- Sakai VG, Maranas JK, Peral I, Copley JRD (2008) Dynamics of PEO in blends with PMMA: study of the effects of blend composition via quasi-elastic neutron scattering. *Macromolecules* 41:3701–3710
- Sengwa RJ, Choudhary S (2016) Dielectric dispersion and relaxation in polymer blend based nanodielectric film. *Macromol Symp* 362:132–138
- Choudhary S (2018) Effects of amorphous silica nanoparticles and polymer blend compositions on the structural, thermal and dielectric properties of PEO-PMMA blend based polymer nanocomposites. *J Polym Res* 25:116
- Dionisio M, Fernandes AC, Mano JF, Correia NT, Sousa RC (2000) Relaxation studies in PEO/PMMA blends. *Macromolecules* 33:1002–1011
- Farago B, Chen C, Maranas JK, Kamath S, Colby RH, Pasquale AJ, Long TE (2005) Collective motion in poly(ethylene oxide)/poly(methylmethacrylate) blends. *Phys Rev E* 72:031809 (11pp)
- Brodeck M, Alvarez F, Colmenero J, Richter D (2012) Single chain dynamic structure factor of poly(ethylene oxide) in dynamically asymmetric blends with poly(methyl methacrylate). *Neutron*

- scattering and molecular dynamics simulations. *Macromolecules* 45:536–542
10. Liang B, Tang S, Jiang Q, Chen C, Chen X, Li S, Yan X (2015) Preparation and characterization of PEO–PMMA polymer composite electrolytes doped with nano- Al_2O_3 . *Electrochim Acta* 169:334–341
 11. Lim YS, Jung H-A, Hwang H (2018) Fabrication of PEO-PMMA- LiClO_4 -based solid polymer electrolytes containing silica aerogel particles for all-solid-state lithium batteries. *Energies* 11:2559
 12. Kanimozhi G, Vinoth S, Harish K, Srinadhu ES, Satyanarayana N (2018) Conductivity and dielectric permittivity studies of KI-based nanocomposite (PEO/PMMA/KI/I₂/ZnO nanorods) polymer solid electrolytes. *Polym Compos.* <https://doi.org/10.1002/pc.25123>
 13. Sengwa RJ, Choudhary S, Dhatarwal P (2015) Influence of ultrasonic- and microwave-irradiated preparation methods on the structural and dielectric properties of (PEO–PMMA)– LiCF_3SO_3 -x wt% MMT nanocomposite electrolytes. *Ionics* 21:95–109
 14. Dhatarwal P, Sengwa RJ (2017) Dielectric and electrical characterization of (PEO–PMMA)– LiBF_4 -EC plasticized solid polymer electrolyte films. *J Polym Res* 24:135
 15. Sengwa RJ, Dhatarwal P, Choudhary S (2018) Study of time-ageing effect on the ionic conduction and structural dynamics in solid polymer electrolytes by dielectric relaxation spectroscopy. *Solid State Ionics* 324:247–259
 16. Venkatesan S, Liu I-P, Lin J-C, Tsai M-H, Teng H, Lee Y-L (2018) Highly efficient quasi-solid-state dye-sensitized solar cells using polyethylene oxide (PEO) and poly(methyl methacrylate) (PMMA)-based printable electrolytes. *J Mater Chem A* 6:10085–10094
 17. Xue Z, He D, Xie X (2015) Poly(ethylene oxide)-based electrolytes for lithium-ion batteries. *J Mater Chem A* 3:19218–19253
 18. Sengwa RJ, Choudhary S (2014) Dielectric properties and fluctuating relaxation processes of poly(methyl methacrylate) based polymeric nanocomposite electrolytes. *J Phys Chem Solids* 75:765–774
 19. Pal P, Ghosh A (2018) Influence of TiO_2 nano-particles on charge carrier transport and cell performance of PMMA– LiClO_4 based nano-composite electrolytes. *Electrochim Acta* 260:157–167
 20. Dhatarwal P, Sengwa RJ, Choudhary S (2019) Effectively improved ionic conductivity of montmorillonite clay nanoplatelets incorporated nanocomposite solid polymer electrolytes for lithium ion-conducting devices. *SN Appl Sci* 1:112
 21. Glynos E, Petropoulou P, Mygiakis E, Nega AD, Pan W, Papoutsakis L, Giannelis EP, Sakellariou G, Anastasiadis SH (2018) Leveraging molecular architecture to design new, all-polymer solid electrolytes with simultaneous enhancement in modulus and ionic conductivity. *Macromolecules* 51:2542–2550
 22. Choudhary S, Sengwa RJ (2017) Effects of different inorganic nanoparticles on the structural, dielectric and ion transportation properties of polymers blend based nanocomposite solid polymer electrolytes. *Electrochim Acta* 247:924–941
 23. Dhatarwal P, Choudhary S, Sengwa RJ (2018) Electrochemical performance of Li^+ -ion conducting solid polymer electrolytes based on PEO–PMMA blend matrix incorporated with various inorganic nanoparticles for the lithium ion batteries. *Compos Commun* 10:11–17
 24. Guo JZ, Song K, Liu C (2019) Polymer-based multifunctional nanocomposites and their applications. Elsevier Inc., Amsterdam
 25. Kashfipour MA, Mehra N, Zhu J (2018) A review on the role of interface in mechanical, thermal, and electrical properties of polymer composites. *Adv Compos Hybrid Mater* 1:415–439
 26. Aqeel SM, Huang Z, Walton J, Baker C, Falkner D'L, Liu Z, Wang Z (2018) Polyvinylidene fluoride (PVDF)/polyacrylonitrile (PAN)/carbon nanotube nanocomposites for energy storage and conversion. *Adv Compos Hybrid Mater* 1:185–192
 27. Wei H, Gu H, Guo J, Cui D, Yan X, Liu J, Cao D, Wang X, Wei S, Guo Z (2018) Significantly enhanced energy density of magnetite/polypyrrole nanocomposite capacitors at high rates by low magnetic fields. *Adv Compos Hybrid Mater* 1:127–134
 28. Chen J, Liu B, Gao X, Xu D (2018) A review of the interfacial characteristics of polymer nanocomposites containing carbon nanotubes. *RSC Adv* 8:28048
 29. Tan D, Irwin P (2011) Polymer based nanodielectric composites in, advances in ceramics: electric and magnetic ceramics, bioceramics, ceramics and environment ed. by Sikalidis C., Intechopen, London
 30. Daily CS, Sun W, Kessler MR, Tan X, Bowler N (2014) Modeling the interphase of a polymer-based nanodielectric. *IEEE Trans Dielectric Electrical Insul* 21:488–496
 31. Tanaka T, Vaughan AS (2017) Tailoring of nanocomposite dielectrics: from fundamentals to devices and applications. Pan Stanford Publishing Pte. Ltd., Singapore
 32. Choudhary S, Sengwa RJ (2019) Investigation on structural and dielectric properties of silica nanoparticles incorporated poly(ethylene oxide)/poly(vinyl pyrrolidone) blend matrix based nanocomposites. *J Inorg Organomet Polym.* <https://doi.org/10.1007/s10904-018-1034-1>
 33. Choudhary S, Sengwa RJ (2018) ZnO nanoparticles dispersed PVA–PVP blend matrix based high performance flexible nanodielectrics for multifunctional microelectronic devices. *Curr Appl Phys* 18:1041–1058
 34. Mathur V, Arya PK (2018) Dynamic mechanical analysis of PVC/ TiO_2 nanocomposites. *Adv Compos Hybrid Mater* 1:741–747
 35. Morsi MA, Rajeh A, Menazea AA (2019) Nanosecond laser-irradiation assisted the improvement of structural, optical and thermal properties of polyvinyl pyrrolidone/carboxymethyl cellulose blend filled with gold nanoparticles. *J Mater Sci Mater Electron.* <https://doi.org/10.1007/s10854-018-0545-4>
 36. Ambrosio R, Carrillo A, Mota ML, Torre K, Torrealba R, Moreno M, Vazquez H, Flores J, Vivaldo I (2018) Polymeric nanocomposites membranes with high permittivity based on PVA–ZnO nanoparticles for potential applications in flexible electronics. *Polymers* 10:1370
 37. Sengwa RJ, Choudhary S (2017) Dielectric and electrical properties of PEO– Al_2O_3 nanocomposites. *J Alloys Compd* 701:652–659
 38. Choudhary S, Sengwa RJ (2017) Morphological, structural, dielectric and electrical properties of PEO–ZnO nanodielectric films. *J Polym Res* 24:54
 39. Choudhary S (2018) Characterization of amorphous silica nanofiller effect on the structural, morphological, optical, thermal, dielectric and electrical properties of PVA–PVP blend based polymeric nanocomposites for their flexible nanodielectric applications. *J Mater Sci Mater Electron* 29:10517–10534
 40. Choudhary S, Sengwa RJ (2015) Dielectric dispersion and relaxation studies of melt compounded poly(ethylene oxide)/silicon dioxide nanocomposites. *Polym Bull* 72:2591–2604
 41. Choudhary S (2017) Dielectric dispersion and relaxations in (PVA–PEO)–ZnO polymer nanocomposites. *Physica B* 522:48–56
 42. Choudhary S (2017) Structural and dielectric properties of (PEO–PMMA)– SnO_2 nanocomposites. *Compos Commun* 5:54–63
 43. Sengwa RJ, Choudhary S, Sankhla S (2010) Dielectric properties of montmorillonite clay filled poly(vinyl alcohol)/poly(ethylene oxide) blend nanocomposites. *Compos Sci Technol* 70:1621–1627
 44. Choudhary S (2018) Structural, morphological, thermal, dielectric, and electrical properties of alumina nanoparticles filled PVA–PVP blend matrix-based polymer nanocomposites. *Polym Compos* 39: E1788–E1799
 45. Choudhary S (2018) Influence of Al_2O_3 nanoparticles on the dielectric properties and structural dynamics of PVA-PEO blend based nanocomposites. *Indian J Chem Technol* 25:51–60
 46. Evans KA (1996) The manufacture of alumina and its use in ceramics and related applications. *Key Eng Mater* 122–124:489–526

47. Tok AIY, Boey FYC, Zhao XL (2006) Novel synthesis of Al₂O₃ nano-particles by flame spray pyrolysis. *J Mater Process Technol* 178:270–273
48. Wang Y, Shih K, Jiang X (2012) Phase transformation during the sintering of γ -alumina and the simulated Ni-laden waste sludge. *Ceram Int* 38:1879–1886
49. Luo Y, Wu G, Liu J, Peng J, Zhu G, Gao G (2014) Investigation of temperature effects on voltage endurance for polyimide/Al₂O₃ nanodielectrics. *IEEE Trans Dielect Elect Insul* 21:1824–1834
50. Bhavsar S, Patel GB, Singh NL (2018) Investigation of optical properties of aluminium oxide doped polystyrene polymer nanocomposite films. *Physica B* 533:12–16
51. Kaybal HB, Ulus H, Demir O, Şahin ÖS, Avc A (2018) Effects of alumina nanoparticles on dynamic impact responses of carbon fiber reinforced epoxy matrix nanocomposites. *Eng Sci Technol Int J* 21:399–407
52. Zhou P, Wang S, Tao C, Guo X, Hao L, Shao Q, Liu L, Wang Y-P, Chu W, Wang B, Luo S-Z, Guo Z (2018) PAA/alumina composites prepared with different molecular weight polymers and utilized as support for nickel-based catalyst. *Adv Polym Technol* 37:2325–2335
53. Mallakpour S, Khadem E (2015) Recent development in the synthesis of polymer nanocomposites based on nano-alumina. *Prog Polym Sci* 51:74–93
54. Sengwa RJ, Choudhary S (2017) Nonlinear enhancement of the dielectric properties of PVA-Al₂O₃. *Adv Mater Process* 2:280–287
55. Das S, Ghosh A (2015) Ion conduction and relaxation in PEO-LiTFSI-Al₂O₃ polymer nanocomposite electrolytes. *J Appl Phys* 117:174103
56. Bandara TMWJ, Karunathilaka DGN, Ratnasekera JL, Silva LAD, Herath AC, Mellander BE (2017) Electrical and complex dielectric behaviour of composite polymer electrolyte based on PEO, alumina and tetrapropylammonium iodide. *Ionics* 23:1711–1719
57. Fullerton-Shirey SK, Maranas JK (2010) Structure and mobility of PEO/LiClO₄ solid polymer electrolytes filled with Al₂O₃ nanoparticles. *J Phys Chem C* 114:9196–9206
58. Arjomandi J, Lee JY, Movafagh R, Moghanni-Bavil-Olyaei H, Parvin MH (2018) Polyaniline/aluminum and iron oxide nanocomposites supercapacitor electrodes with high specific capacitance and surface area. *J Electroanal Chem* 810:100–108
59. Masoud EM, El-Bellihi A-A, Bayoumy WA, Mousa MA (2013) Organic–inorganic composite polymer electrolyte based on PEO–LiClO₄ and nano-Al₂O₃ filler for lithium polymer batteries: dielectric and transport properties. *J Alloys Compd* 575:223–228
60. Kiran Kumar K, Ravi M, Pavani Y, Bhavani S, Sharma AK, Narasimha Rao VVR (2014) Investigations on PEO/PVP/NaBr complexed polymer blend electrolytes for electrochemical cell applications. *J Membr Sci* 454:200–211
61. Mishra MK, Moharana S, Behera B, Mahaling RN (2017) Surface functionalization of BiFeO₃: a pathway for the enhancement of dielectric and electrical properties of poly(methyl methacrylate)–BiFeO₃ composite films. *Front Mater Sci* 11:82–91
62. Pan Z, Yao L, Zhai J, Shen B, Wang H (2017) Significantly improved dielectric properties and energy density of polymer nanocomposites via small loaded of BaTiO₃ nanotubes. *Compos Sci Technol* 147:30–38
63. Kaur R, Samra KS (2018) Electrical and mechanical behavior of polymethyl methacrylate/cadmium sulphide composites. *Physica B* 538:29–34
64. Maji P, Choudhary RB, Majhi M (2018) Polymeric phase change nanocomposite (PMMA/Fe:ZnO) for electronic packaging application. *Appl Phys A Mater Sci Process* 124:70
65. Mao F, Shi Z, Wang J, Zhang C, Yang C, Huang M (2018) Improved dielectric permittivity and retained low loss in layer-structured films via controlling interfaces. *Adv Compos Hybrid Mater* 1:548–557
66. Huang YH, Schadler LS (2017) Understanding the strain-dependent dielectric behaviour of carbon black reinforced natural rubber - an interfacial or bulk phenomenon. *Compos Sci Technol* 142:91–97
67. Kontos GA, Soulintzis AL, Karahaliou PK, Psarras GC, Georga SN, Krontiras CA, Pisanias MN (2007) Electrical relaxation dynamics in TiO₂-polymer matrix composites. *Express Polym Lett* 1:781–789
68. Mukherjee PS, Das AK, Dutta B, Meikap AK (2017) Role of silver nanotube on conductivity, dielectric permittivity and current voltage characteristics of polyvinyl alcohol-silver nanocomposite film. *J Phys Chem Solids* 111:266–273
69. Sinha S, Chatterjee SK, Ghosh J, Meikap AK (2017) Analysis of the dielectric relaxation and ac conductivity behavior of polyvinyl alcohol-cadmium selenide nanocomposite films. *Polym Compos* 38:287–298
70. Rajeh A, Morsi MA, Elashmawi IS (2019) Enhancement of spectroscopic, thermal, electrical and morphological properties of polyethylene oxide/carboxymethyl cellulose blends: combined FT-IR/DFT. *Vacuum* 159:430–440
71. Choudhary S (2018) Structural, optical, dielectric and electrical properties of (PEO–PVP)–ZnO nanocomposites. *J Phys Chem Solids* 121:196–209
72. Choudhary S (2016) Characterization of SiO₂ nanoparticles dispersed (PVA–PEO) blend based nanocomposites as the polymeric nanodielectric materials. *Indian J Eng Mater Sci* 23:399–410
73. Choudhary S, Sengwa RJ (2017) Role of doped ZnO nanoparticles as polymer chain segmental motion exciter in PVA–ZnO nanocomposites investigated by dielectric relaxation spectroscopy. *Adv Mater Process* 2:315–324
74. Choudhary S, Sengwa RJ (2016) Anomalous dielectric behaviour of poly(vinyl alcohol)-silicon dioxide (PVA–SiO₂) nanocomposites. *AIP Conf Proc* 1728:020420
75. Xu F, Zhang H, Jin L, Li Y, Li J, Gan G, Wei M, Li M, Liao Y (2018) Controllably degradable transient electronic antennas based on water-soluble PVA/TiO₂ films. *J Mater Sci* 53:2638–2647
76. Irimia-Vladu M (2014) “Green” electronics: biodegradable and biocompatible materials and devices for sustainable future. *Chem Soc Rev* 43:588–610
77. Deshmukh K, Ahamed MB, Sadasivuni KK, Ponnamma D, Al-Ali AlMaadeed M, Deshmukh RR, Pasha SKK, Polu AR, Chidambaram K (2017) Fumed SiO₂ nanoparticle reinforced biopolymer blend nanocomposites with high dielectric constant and low dielectric loss for flexible organic electronics. *J Appl Polym Sci* 134:44427
78. Feig VR, Tran H, Bao Z (2018) Biodegradable polymeric materials in degradable electronic devices. *ACS Cent Sci* 4:337–348
79. Li R, Wang L, Yin L (2018) Materials and devices for biodegradable and soft biomedical electronics. *Materials* 11:2108